

On the Feasibility of Securing Vehicle-Pavement Interaction

WEI SUN*, The Ohio State University, Columbus, USA

KANNAN SRINIVASAN, The Ohio State University, Columbus, USA

Road surface information (e.g., smooth road or bumpy road with potholes or bumps) is important for safe driving (i.e., it's necessary to be aware of the road surface conditions during driving). However, the high-cost sensor (e.g., LiDAR and camera) based road surface sensing approaches cannot work properly in inclement weather conditions (e.g., fogging and snowing) due to the line-of-sight requirement. The low-cost and ubiquitous smartphone-based road surface sensing approach is not reliable and safe to use, since it relies on the vibration of the vehicle body to sense the road surface (i.e., the vehicle's tires need to touch the bumps on the road surface). *Can we automate the contact-free road surface sensing with low-cost sensors for safe driving without requiring the vehicle's tires to touch the bumps on the road surface?*

In this paper, we propose Tago, a system that can achieve contact-free road surface sensing with commodity passive RFID tags. Instead of deploying RFID tags or readers along the road or lamp post (i.e., infrastructure-based deployment), we deploy the reader inside of the vehicle and attach the tag and the reader's antenna at the front end of the vehicle like the vehicle's headlights (i.e., infrastructure-free deployment). However, there is a great challenge to obtain the clean reflection from the road surface, since the reflection may be drown in the backscattered signals due to multipath effect. Moreover, it is not reliable to use the composite signals received at the reader to sense the road surface conditions. Therefore, we first comprehensively analyse the variation of composite signals received at the reader. Then, we propose a signal cancellation approach to extract the clean reflections from the road surface, such that we can accurately sense the road surface conditions for safe driving. Our experiments with different vehicles (e.g., Honda Civic Frankenfish, Folsom, Flutter and CR-V Warner) driven on different roadways (e.g., urban and residential area) show that Tago can effectively sense the road surface information.

CCS Concepts: • Human-centered computing → Ubiquitous and mobile computing; • Security and privacy → Human and societal aspects of security and privacy.

Additional Key Words and Phrases: Commodity Passive RFID Tag, Road Surface Sensing, Contact-Free Sensing, Safe Driving

ACM Reference Format:

Wei Sun and Kannan Srinivasan. 2022. On the Feasibility of Securing Vehicle-Pavement Interaction. *Proc. ACM Interact. Mob. Wearable Ubiquitous Technol.* 6, 1, Article 29 (March 2022), 24 pages. <https://doi.org/10.1145/3517230>

1 INTRODUCTION

1.1 Why Do We Need Road Surface Sensing?

The bad road surface conditions (e.g., bumps or potholes on the road surface) are caused by severe and dynamic weather conditions, unexpected and heavy traffic loads and the normal wear/tear. Even though the governments around the world spend a lot of money on maintaining the quality of the roadways, the bad road surface conditions are still hazardous to drivers and pedestrians [19]. It is difficult for the governments to maintain the good quality

*Corresponding authors

Authors' addresses: Wei Sun, The Ohio State University, Columbus, USA, sun.1868@osu.edu; Kannan Srinivasan, The Ohio State University, Columbus, USA, srinivasan.115@osu.edu.

Permission to make digital or hard copies of all or part of this work for personal or classroom use is granted without fee provided that copies are not made or distributed for profit or commercial advantage and that copies bear this notice and the full citation on the first page. Copyrights for components of this work owned by others than ACM must be honored. Abstracting with credit is permitted. To copy otherwise, or republish, to post on servers or to redistribute to lists, requires prior specific permission and/or a fee. Request permissions from permissions@acm.org.

© 2022 Association for Computing Machinery.

2474-9567/2022/3-ART29 \$15.00

<https://doi.org/10.1145/3517230>



Fig. 1. Tago's architecture. The RFID reader's antenna and RFID tag are attached at the front end of the vehicle to achieve contact-free road surface sensing. Specifically, the reader's antennas (i.e., Tx antenna and Rx antenna) are attached at the front end of the vehicle and the tag is attached on the reader's antenna. The shadow area (i.e., shown in the left figure) in front of the vehicle indicates the RF beam transmitted from the reader's antenna. So, the sensing area of Tago is the road surface in front of the vehicle. Specifically, the backscattered signals reflected off the road surface will be analysed to sense bumps or potholes on the road surface.

of roadways in the long term due to the limited municipal budget and transportation agencies. Also, the process of road maintenance will last a long period of time, which will further cause the traffic congestion in some main roadways. So, we cannot expect the roadways to be smooth all the time. These bad road surface conditions could approximately cause \$3 billions in property damage every year [2], and degrade the efficiency of the vehicles (e.g., waste the fuel) as the vehicle is driven on bumpy road instead of the smooth road. The bad road surface conditions become even worse for the autonomous driving systems, which require us to design the robust and reliable machine learning models to capture the complex road surface conditions. Therefore, it is necessary for the vehicular systems or drivers to be aware of the road surface conditions for *economic and safe driving*. This is also why we have eye-on-road driving guideline [17].

1.2 Problems of Prior Art on Road Surface Sensing

Camera, radar or LiDAR-based road surface sensing. The straightforward solution is to instrument the high-cost and advanced sensors (e.g., camera, radar or LiDAR sensor) on the vehicle [1] to accurately sense the road surface conditions, which have been employed by modern autonomous vehicles (e.g., Waymo [39]). However, these advanced sensors are expensive. More importantly, camera and LiDAR sensors require the line-of-sight to work properly, which is not reliable in inclement weather conditions (e.g., fogging and snowing).

Smartphone or crowd-sourced smartphone-based road surface sensing. Recently, low-cost IMU sensors (e.g., GPS, magnetometer, gyroscope and accelerometer) embedded in the smartphone are leveraged to sense the road surface conditions [9, 21]. However, these smartphone-based or crowd-sourced smartphone-based approaches cannot provide reliable road surface sensing, since the smartphone's MEMS sensors are prone to noise, drifts and biases. More importantly, they cannot achieve contact-free road surface sensing for safe driving and alert the drivers of the hazardous road conditions ahead, since they sense the road surface based on the vibration of the vehicle's body which requires the vehicle's tires to touch the bumps.

Therefore, it is critical to achieve the low-cost, ubiquitous and contact-free road surface sensing for safe driving. More details of prior art on road surface sensing can be found in §2. Next, we illustrate why we choose commodity passive RFID for road surface sensing.

1.3 Why Do We Choose Commodity Passive RFID for Road Surface Sensing?

Recently, the commodity passive RFID system has been widely exploited for ubiquitous sensing (e.g., touch sensing [16, 33], soil moisture sensing [31], food/liquid sensing [12, 36], gesture recognition [14, 34, 35], etc.) due

to its low cost and small form factor. Note that the ubiquitous smartphones can be used as RFID reader, which is exploited in [5, 8]. More importantly, since the commodity passive RFID relies on the radio frequency signals to sense the objects (e.g., road surface), it can inform the driver of the hazardous road conditions ahead before the vehicle’s tires touch the bumps on the road surface. Therefore, we believe commodity passive RFIDs are the good choice to automate contact-free road surface sensing for safe driving. The rationale of using RFIDs is they are low-cost and they can be the complement of camera/lidar/radar systems in NLOS scenarios. We think that the active tag needs the battery, which requires us to replace it regularly. So, it is not convenient. Moreover, Tago’s design is not inherited from the tag. So, Tago’s design can be general to any backscatter sensors including the active tags. The advanced sensors such as Lidar sensors, which cannot provide the large enough signal wavelength to penetrate fog, rain and snow [10, 18, 22, 24]. Typically, the Lidar signal has the wavelength smaller than 0.01mm. Fog particles have the size of 10 to 15mm and rain drops have the size of 0.5 to 5mm, which are larger than 0.01mm.

1.4 Tago’s Design

In this paper, we propose Tago, a system that can sense the road surface conditions using the commodity passive RFID system for safe driving. To do so, we deploy the RFID reader in the vehicle and attach the RFID tags at the front end of the vehicle to achieve contact-free sensing as shown in Fig. 1. However, there are three great challenges to build a functional system. First, to achieve the contact-free sensing, we cannot attach RFID tags on the road surface like the other RFID-tagged objects sensing [30, 32, 35]. The other infrastructure-based settings (e.g., deploying reader on the lamp post [3]) are not appropriate in our scenario. Second, the backscattered signals reflected off the road surface will be drown in the direct-path signals, which will degrade the sensing sensitivity if we use composite signals received at reader to sense the road surface. Moreover, the hardware distortion of tags/reader will introduce extra phase offset to the backscattered signals. At last, the bumps can be randomly distributed on the road surface. So, we cannot use only one tag to reliably sense these bumps due to the orientation sensitivity of commodity passive RFID tags.

To this end, we will first comprehensively analyse above system settings to exploit the variation of reflections from the road surface. It turns out that we cannot just use the composite signals received at the reader to sense the road surface conditions. So, we propose a window-sized signal cancellation approach to obtain the weak reflection from the road surface (i.e., an emerging technique put forward in recent years [43?]), whereby cancelling out the reflections from other objects (e.g., vehicle’s body and curb). Note that the pedestrians on the sidewalk and the other vehicles passing by will not be captured by the tags attached at the front end of the vehicle (as shown in §6), since we harness the orientation sensitivity of RFID system [40] by facing the tag and reader’s antenna to the road surface. We also need to mitigate the hardware imperfections of tag and reader through one-time calibration. Since the commodity passive RFID system is orientation-sensitive, we can deploy two tags on the vehicle (like the vehicle’s headlights) to detect the randomly distributed bumps on the road surface.

Result. We built a prototype of Tago with USRP N210 as the RFID reader and the general-purpose commodity passive RFID tags. The extensive experiments show that Tago can accurately sense the road surface conditions. We deploy the prototype of Tago on different vehicles (i.e., Honda Civic Flutter, Frankenfish, Folsom and CR-V Warner). We do the experiments in our campus road, residential area and urban area. The experimental results show the capability of Tago on contact-free road surface sensing. More details can be found in Sec. 6.

Limitation. Our RFID-based contact-free road surface sensing system marks an important step to shrink the gap between the contact and contact-free road surface sensing for safe driving. Nonetheless, we will discuss some limitations (e.g., sensing range and road surface profiling) of Tago’s design in Sec. 7.

Contributions. We summarize our contributions as follows:

- To the best of our knowledge, Tago is the first contact-free road surface sensing system for safe driving, using commodity passive RFID tags attached at the front end of the vehicle.
- We comprehensively analyse Tago's system settings. Then, we propose a window-sized signal cancellation approach to obtain the weak reflection from the road surface. To achieve reliable sensing, we attach two RFID tags at the front end of the vehicle (like the vehicle's headlights) to sense the randomly distributed bumps on the road surface.
- The extensive experimental results show the efficiency of our Tago's design on road surface sensing, comparing with the state-of-the-art smartphone-based road surface sensing approaches.

Below, we will present the prior work on road surface sensing, which will further comprehend our Tago's low-cost (i.e., in comparison to the cost of camera and LiDAR sensors) and contact-free (i.e., in comparison to the smartphone or crowd-sourced smartphone-based approaches) road surface sensing.

2 RELATED WORK ON ROAD SURFACE SENSING

In the past literature, the road surface sensing has been exploited using different kinds of sensors such as stereo cameras, LiDAR sensors and embedded sensors in the smartphones. So, we will discuss the related work in each of the above sensors-based road surface sensing techniques and illustrate why they are not the good choice for road surface sensing in comparison to Tago.

2.1 Advanced Sensor-Based Road Surface Sensing

The road surface condition can be obtained through the remote sensing, using the satellites or aerial imagery [38]. The remote sensing approaches can achieve large-scale sensing. But, it will cause the high-cost deployment and data collection, especially when we need to frequently update the sensing data. More importantly, this expensive remote sensing approach provides the poor accuracy and cannot provide the fine-grained road surface information (e.g., bumps on the road surface). To improve the sensing accuracy, we can deploy some advanced sensors (e.g., cameras and LiDAR sensors) on the vehicle to sense the road surface [1, 13, 45]. For example, the Automatic Road Analyzer (ARAN [1]) is a vehicle instrumented with many high-quality sensors such as laser, camera and LiDAR to collect the road surface information, by fusing all these sensing data. These sensors can detect and localize the bumps on the road surface, estimate the road grade for efficient fuel usage and measure the dimension of the pothole with high accuracy. The high accuracy is achieved with these expensive sensors, which can just work properly in line-of-sight scenario. The high deployment cost limits its scalability. Moreover, these sensors perform poorly in bad weather conditions such as fogging and snowing. The current autonomous vehicles (e.g., Tesla [28] and Waymo [39]) highly rely on these sensors, since these sensors can provide high accuracy with deep learning algorithms. However, they have high computational complexity and deployment cost to train the deep neural networks in different weather conditions to have robust system.

Obviously, these advanced and expensive sensors could provide high accuracy in line-of-sight scenario. But, they cannot work properly in non-line-of-sight scenario such as fogging and snowing. To alleviate the high cost and achieve ubiquitous sensing, the smartphone-based road surface sensing has been exploited, as the ubiquitous smartphone is embedded with different kinds of IMU sensors such as magnetometer, gyroscope, GPS and accelerometer [9, 11, 21, 25, 46], which can be leveraged to sense the road surface.

2.2 Smartphone or Crowd-Sourced Smartphone-Based Road Surface Sensing

Nericell [21] can monitor road and traffic information with different sensors embedded in the smartphone (e.g., GPS, accelerometer and microphone). P^2 [9] uses the vibration and GPS sensors to assess the road surface conditions. Since the smartphone-based road surface sensing approaches rely on IMU sensors to sense the road surface, there are two main drawbacks using the smartphone to sense road surface conditions as follows:

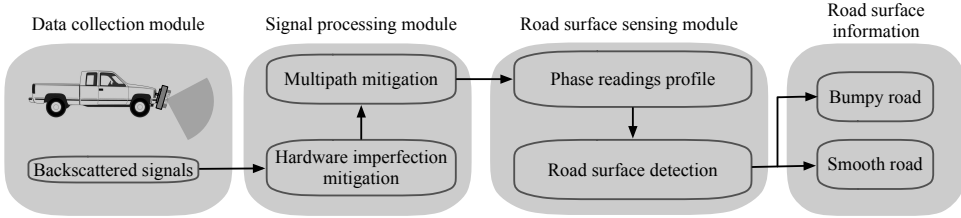


Fig. 2. Tago's operation workflow. Tago mainly consists of signal processing module and road surface sensing module.

- First, the gyroscope and accelerometer integrated into the smartphone are usually used for road surface sensing, which are prone to noise, biases and drifts. For example, gyroscope is usually implemented with Coriolis force [26], which will have the linear output and damping is ignored at the low frequency. When the frequency increases, the damping will gradually become dominant which will cause the oscillation with forced vibration. The frequency offset caused by the drifts will degrade the gyroscope data readings.
- Second, the physical principle of IMU sensors relies on vehicle's body vibration to sense the road surface. So, smartphone-based road surface sensing approach is contact sensing. This violates our design goal of safe driving, which requires the system to alert the driver before the vehicle hits the bump on the road surface. Therefore, it is essential to have contact-free road surface sensing approach.

Later on, the researchers try to improve the smartphone-based road surface sensing, through minimizing the IMU sensor's erroneous and leveraging the concept of crowdsourcing. However, they do not actually achieve contact-free road surface sensing for safe driving. For example, RoadCare [29], [46] and [11] sense the road surface conditions with multiple users' smartphones, which will be uploaded to the central cloud to share these road surface conditions with the other drivers. Actually, they still rely on the vehicle's body vibration to sense the road surface, which cannot achieve the goal of safe driving. Moreover, the crowdsourcing method incurs significant overhead and may raise privacy and incentive issues.

3 TAGO OPERATION

Tago is a road surface sensing system that leverages the commodity passive RFID tags to detect the bumps on the road surface. To do so, we attach the reader's antenna and the tag at the front end of the vehicle.

Fig. 2 illustrates Tago's operation workflow, which consists of two main modules: signal processing module and road surface sensing module. Tago's flow of operations includes the following steps: (1) The reader will receive the backscattered signals from the tag; (2) The hardware imperfections of tag and reader's antennas should be mitigated with one-time calibration, since the tag and reader's hardware imperfections are constant; (3) We mitigate the multipath effect through signal cancellation. Since tag and reader's antennas are deployed at the front end of the vehicle as shown in Fig. 1, we mainly cancel the reflections from the vehicle's body, curb and the direct-path signals between reader's antenna and the tag. After the signal cancellation, the remaining part will be the backscattered signal reflected off the road surface; (4) We mainly extract the phase readings from the backscattered signals reflected off the road surface for road surface sensing. To differentiate the bumpy and smooth road surface, we compare the variance of phase readings to the predefined threshold. The bumps or potholes on the road surface will introduce significant phase variation to the phase readings.

In the following, we will elaborate the design details of Tago. We start from modeling the RFID sensing in §4.1. Then, we analyse the difficulties and challenges of contact-free RFID sensing in §4.2. To address the challenges, we propose signal cancellation algorithm to obtain the backscattered signals reflected off the road surface in §4.3. At last, we introduce reliable road surface sensing with two tags in §4.4

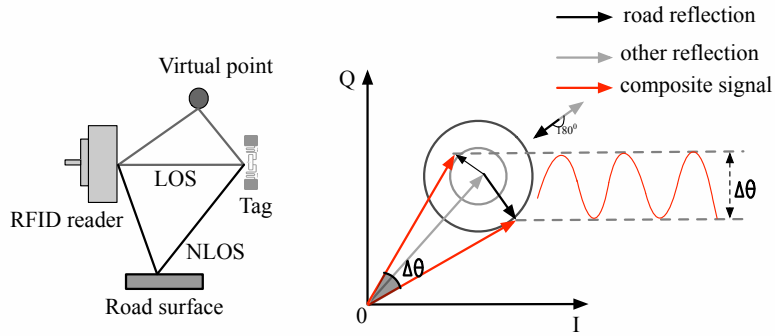


Fig. 3. Left figure shows the back-and-forth signal propagation between the reader and tag (i.e., LOS path), and the NLOS signal propagation reflected off the virtual point (e.g., road curb and vehicle's body) and road surface. Right figure shows the vector representation of signal paths in IQ domain. The variation of road surface will cause the variation of backscattered signals received at the reader.

4 TAGO DESIGN

4.1 Employing RFID Signal for Sensing

Since the commodity passive RFID tags are battery-free, they need to be activated by the external reader through the high-power signals (i.e., continuous wave). Let's assume the transmitted signal from the reader is $S_{rt} = |S_{rt}| e^{j\theta_r}$ (θ_r denotes the phase offset due to the reader's hardware imperfection), which will be propagated to the nearby tags. The tag will receive signals $S_t = S_{rt} h_{rt} h_t$, $h_{rt} = |h_{rt}| e^{j\theta_{rt}}$, $h_t = |h_t| e^{j\theta_t}$, where h_{rt} denotes the wireless channel from the reader to the tag and h_t denotes the tag's antenna gain. Suppose that the reflection coefficient is $\alpha = |\alpha| e^{j\theta_\alpha}$, which is a constant value given the specific RFID tag. The received signals at the tag will be backscattered to the reader through ON-OFF keying modulation. Then, the reader will receive tag's reflections $S_{r'} = S_t \alpha h_t h_{tr} = S_{rt} \alpha h_t^2 h_a^2 = |S_{rt} \alpha h_t^2 h_a^2| e^{j(\theta_r + \theta_\alpha + 2\theta_a + 2\theta_t)}$, where $\theta_a = \theta_{rt}$, $\theta_a = \theta_{tr}$ and $h_a = h_{rt} = h_{tr}$ due to the reciprocity property of the wireless channel.

After the reader receives the backscattered signals from the tag, we can extract the signal strength and phase. The received signal strength of the backscattered signal is denoted as follows:

$$\text{Signal strength} = 20 \log |S_{r'}| = 20 \log |S_{rt}| + 20 \log |\alpha| + 40 \log |h_a| + 40 \log |h_t|$$

The received signal phase of the backscattered signal is denoted as follows:

$$\text{Signal phase} = \theta_r + \theta_\alpha + 2\theta_a + 2\theta_t$$

Since the phase readings can provide more finer resolution than the amplitude readings [20, 30, 32, 35, 40, 42], most of the work employs the phase readings to do RFID-based sensing. So, we will also leverage the signal phase extracted from tag's backscattered signals to achieve road surface sensing. Note that the extracted signal phase from the backscattered signals is related to the hardware imperfection of the tag (i.e., θ_t , θ_α) and reader (i.e., θ_r), which will be addressed in §4.3. Below, we will address the challenge of enabling contact-free RFID sensing.

4.2 Analysing the Impacted Factors on Contact-Free Road Surface Sensing

Instead of deploying the tags or reader on existing infrastructure (e.g., lamp posts along the road), we attach the reader's antenna and tag at the front end of the vehicle to achieve contact-free road surface sensing. From the above discussion, we can see that there are two types of backscattered signals between the reader and the

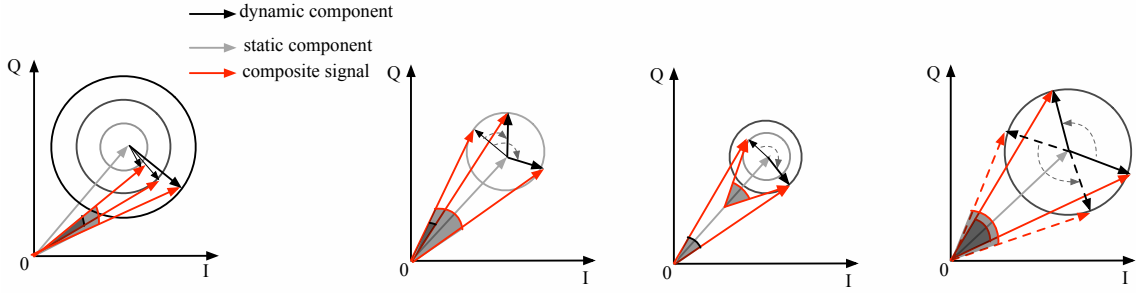


Fig. 4. The impacted factors on using composite signals to sense the road surface conditions. The leftmost figure shows that the amplitude variation of the dynamic component affects the phase variation of the composite signals. The second figure shows that the phase variation of dynamic component will affect the phase variation of the composite signals. The third figure shows that the amplitude of the static component affects the phase variation of the composite signals. The size of circle indicates the amplitude of the dynamic component. The rightmost figure shows the location of the bump or pothole on the road surface will affect the phase variation of the composite signals.

tag: line-of-sight (LOS) signals and non-line-of-sight (NLOS) signals as shown in Fig. 3. The signals directly propagated between the reader's antenna and the tag indicate the LOS path. There are some other objects (e.g., vehicle's body) which can reflect the signals. We regard these objects as a virtual point. The virtual point and road surface cause the NLOS signal transmission.

The vector representation of LOS and NLOS signal paths are shown in Fig. 3. The LOS path and the signal path traversing over the virtual point can be seen as the static component. The reflection from the road surface can be regarded as the dynamic component due to the change of road surface (e.g., from smooth to bumpy). Since the road surface can change, the backscattered signals from the road surface will change (i.e., amplitude or phase variation) due to the different propagation distance. We use the size of the circle in Fig. 3 to indicate the signal amplitude reflected off the road surface. The reader will just receive the composite signals. When the phase difference between the static component and the average dynamic component is 180° as shown in Fig. 3, we can see the obvious phase variation (i.e., $\Delta\theta$) of the composite signals. However, it is difficult to know if this phase variation is enough to sense the road surface conditions. Next, we present factors that will affect the sensing ability of using composite signals for road surface sensing.

Fig. 4 shows the impacted factors that can affect the phase variation of the composite signals received at the reader. From the leftmost figure, we can see that the amplitude of the signals reflected off the road surface will affect the phase variation of the composite signals received at the reader. As the amplitude variation of the dynamic component becomes larger, the phase variation of the composite signals becomes larger. However, the amplitude of the signals reflected off the road surface depends on the material contents of the road surface and the distance between the reader's antenna and the road surface. The second figure shows that the phase variation of the dynamic component will affect the phase variation of the composite signals. As the phase variation of dynamic component becomes larger, the phase variation of the composite signals becomes larger. The third figure shows that the amplitude of the static component will affect the phase variation of the composite signals. As the amplitude of the static component becomes smaller, the phase variation of composite signals becomes larger. However, it is difficult to control above three factors to maximize the phase variation of the composite signals received at the reader [41]. Note, the location of bumps or potholes on the road surface will also affect the

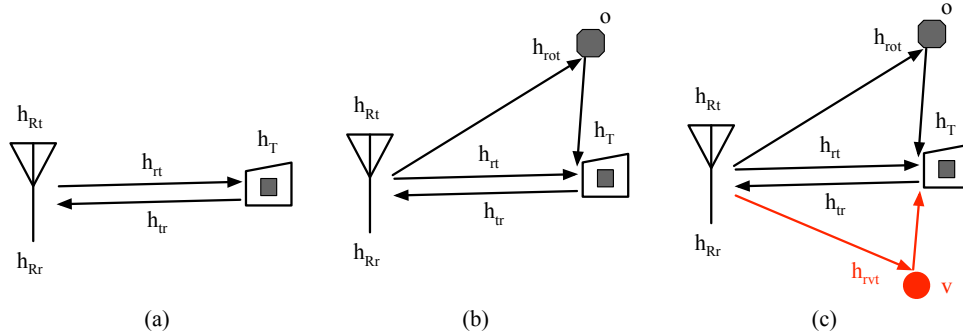


Fig. 5. Modeling the propagation of the backscattered signal. (a) When there are no other objects around the commodity passive RFID system, we just consider line-of-sight propagation between the reader and tag. (b) When there are other objects around the commodity passive RFID system, we regard o as the other reflectors. We should consider the propagation path traversing over o from reader to the tag. (c) Extracting the reflection from the road surface (i.e., denoted as v) through the cancellation. Note that our objective is to obtain channel h_{rot} for road surface sensing.

variation of composite signals as shown in the rightmost figure. So, we need to directly extract the reflections from the road surface to obtain the road surface information.

Instead of maximizing the phase variation of the composite signals by introducing another tag to harness the tag-tag coupling effect (e.g., TagSMM [41] is designed for vibration sensing), we propose to extract the clean backscattered signals reflected off the road surface to sense the road surface conditions. This is because TagSMM need carefully deploy non-target tag to harness the coupling effect between the target tag and non-target tag, which is not reliable when both of the tags are attached at the front end of the vehicle due to the vibration of the vehicle's body. RF-EAR [44] leverages the Orthogonal Matching Pursuit algorithm to characterize different vibration sources by scaling the different factors for different vibration sources, which is designed for vibration sensing. In Tago, the tag and reader's antenna are co-located on the front end of the vehicle (i.e., infrastructure-free), which is different from the existing infrastructure-based RFID sensing systems.

4.3 Enabling Contact-Free Road Surface Sensing through Signal Cancellation

To obtain the clean reflections from the road surface, we propose the backscattered signal cancellation approach to sense the road surface.

Since we deploy the reader's antenna and tags at the front end of the vehicle, the tag will modulate the composite signal from the reader (i.e., signals transmitted from reader's transmit antenna) and the background reflectors (i.e., signals reflected off the different objects around the tag). Then, the composite signal will be reflected off the tag through ON-OFF keying modulation. The reflections from the bump on the road surface will be drowned in the background reflections, thereby it's essential to disentangle the road surface reflections from the background reflections. This is because the direct-link signals will be the dominant due to Tago's settings.

Modeling backscatter communication in LOS. We first present the case when there are no reflectors around commodity passive RFID system (i.e., LOS setting) as shown in Fig. 5(a). As mentioned in Sec. 4.1, in commodity passive RFID system, the reader should initialize the communication and activate the tags by sending the constant continuous wave (i.e., cw). After the tag is activated, it will respond by backscattering the cw signals with ON-OFF keying modulation. Let's assume the reader sends an request x (i.e., complex scalar value) to the tag within its communication range. The tag will backscatter the received signal through ON-OFF keying modulation.

So, the reader will receive the backscattered signal as follows:

$$y_d = h_{Rr}h_{tr}h_Th_{rt}h_{Rt}zx + h_{Rr}h_{rr}h_{Rt}x, \quad (1)$$

where h_{tr} denotes the wireless channel from tag to reader's receive antenna, and h_{rr} denotes the channel from the reader's transmit antenna to receive antenna. h_{rt} denotes the channel from reader's transmit antenna to tag. z denotes the data transmitted by tag. We use h_{Rt} , h_{Rr} and h_T to denote the hardware distortion at reader's transmit antenna, receive antenna and tag respectively. $h_{Rr}h_{rr}h_{Rt}x$ represents the self-interfered signals received at the reader's receive antenna. The impinged signals on the tag body are $h_{rt}h_{Rt}x$. Since the passive RFID tag simply backscatters the impinged signals from the reader, we only consider h_T once. Then, the backscattered signals received by the reader's receive antenna are $h_{Rr}h_{tr}h_Th_{rt}h_{Rt}x$. Note that the RFID reader is capable to do self-interference cancellation to eliminate the signal leakage at reader. Therefore, the reader will receive the following signal:

$$\begin{aligned} y_d &= h_{Rr}h_{tr}h_Th_{rt}h_{Rt}zx + h_{rr}h_{Rt}h_{Rr}x - h_{rr}h_{Rt}h_{Rr}x \\ &= h_{Rr}h_{tr}h_Th_{rt}h_{Rt}zx \end{aligned} \quad (2)$$

Backscatter communication in NLOS. When there are other objects (e.g., vehicle's body or curb) around the commodity passive RFID system. The reader will receive the composite reflections from the tag and other objects as shown in Fig. 5(b). Instead of modulating the signal from the reader, the tag will modulate the composite signal from the reader and other objects. So, the impinged signal on the tag is $h_{rt}h_{Rt}x + h_{rot}h_{Rt}x$, where $h_{rt}h_{Rt}x$ denotes the impinged signal from the reader and $h_{rot}h_{Rt}x$ denotes the impinged signal traversing over the other objects. We use h_{rot} to denote the channel traversing over the other objects from the reader to tag. After the reader cancels out the self-interference signal, the reader will receive the following signal:

$$y_o = h_{Rr}h_{tr}h_Th_{rt}h_{Rt}zx + h_{Rr}h_{tr}h_Th_{rot}h_{Rt}zx. \quad (3)$$

As we can see from the above equation, our objective is to estimate the channel affected by the other objects (e.g., road surface). However, $h_{Rr}h_{tr}h_Th_{rt}h_{Rt}$ will dominate the received signal y_o , which will affect the road surface sensing. Next, we will illustrate how to extract the channel traversing over the road surface through cancellation. **Extracting the reflection from road surface through cancellation.** Since our objective is to obtain the reflections from the road surface, we need to cancel out the reflections from the other objects such as the vehicle's body. Fig. 5(c) shows the signal paths between the reader and tag, when we drive the vehicle on the road. We use v to denote the reflection from the road surface. So, the tag will modulate the impinged signal $h_{rt}h_{Rt}x + h_{rot}h_{Rt}x + h_{rov}h_{Rt}x$ with ON-OFF keying modulation, where $h_{rov}h_{Rt}x$ denotes the signal traversing over the road surface. We use h_{rov} to denote the channel traversing over the road surface from the reader to the tag. After self-interference cancellation, the reader will receive the signal as follows:

$$y_v = h_{Rr}h_{tr}h_Th_{rt}h_{Rt}zx + h_{Rr}h_{tr}h_Th_{rot}h_{Rt}zx + h_{Rr}h_{tr}h_Th_{rov}h_{Rt}zx. \quad (4)$$

The backscattered signals received at the reader mainly consist of two components: the direct reflection and multi-path reflection. For the multi-path reflections from tag to reader, reflected signals from tag come from two sources: directly impinged signals from reader and the other objects' reflections, which will be used by the tag to modulate its own data. For the tag's reflected signals directly coming from the reader, when they are backscattered by the tag over other objects, they are also included in the second component of right side of Eq.(4) due to the reciprocity of dominant and over-the-air wireless channel. For the tag's reflected signals coming from the other objects' reflections, when they are backscattered by the tag over other objects, they become weaker due to multiple attenuation. So, in Eq.(4), we just count the reflections over the other objects once. To demonstrate this, we show the IQ constellation of the backscattered channel before and after signal subtraction in Fig. 6. As

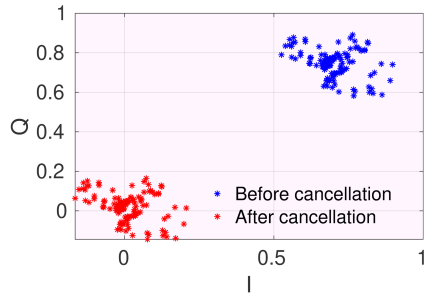


Fig. 6. Backscattered channel in IQ domain before and after dominant signal cancellation in Eq.(4). Note, Eq.(5) shows the signal cancellation process.

we can see, after the signal subtraction, the channel samples are distributed around origin point. This is because we cancel out the dominant contribution from the composite backscattered channel. This indicates that we can ignore the reflections traversing over objects multiple times and the impact of RFIC's impedance due to their weak impact.

Algorithm 1 Road surface sensing with signal cancellation algorithm

Require:

- Commodity RFID passive system and the vehicle;

Ensure:

- The expected channel traversing over the road surface from the reader to tag h_{rot} ;

1: **Distortion mitigation:** Estimating H' and

$$h_{rt} = h_{tr} = \frac{1}{a_{rt}^2} e^{-j2\pi \frac{d_{rt}}{\lambda} \text{ mod } 2\pi},$$

2: **Backscattered signal extraction:** Obtaining the backscattered signals received at the reader

$$y_o = h_{Rr} h_{tr} h_T h_{rt} h_{Rt} zx + h_{Rr} h_{tr} h_T h_{rot} h_{Rt} zx;$$

3: **Real-time backscattered signal cancellation:** Obtaining the expected channel through cancellation

$$y'_v = y_v - y_o = h_{Rr} h_{tr} h_T h_{rot} h_{Rt} zx,$$

where y_v is obtained through equation (4);

4: Return the channel estimation $h_{rot} = \frac{h_o}{H' \frac{1}{d_{rt}^2} e^{-j2\pi \frac{d_{rt}}{\lambda} \text{ mod } 2\pi}}$;

To extract the reflections from the road surface, we need to do the subtraction as follows:

$$y'_v = y_v - y_o = h_{Rr} h_{tr} h_T h_{rot} h_{Rt} zx, \quad (5)$$

where $h_o = h_{Rr} h_{tr} h_T h_{rot} h_{Rt}$ will be extracted through the backscattered channel estimation. Since we deploy tag and reader's antenna at the front end of the vehicle, the reflections from the vehicle's body are quite stable. So, we can do above subtraction, especially in the outdoor environment. Note that the above subtraction can also cancel out the effect of engine's vibration. Since our objective is to obtain the channel h_{rot} , we still need to eliminate the impact of hardware distortion and the line-of-sight propagation between the reader and tag. The

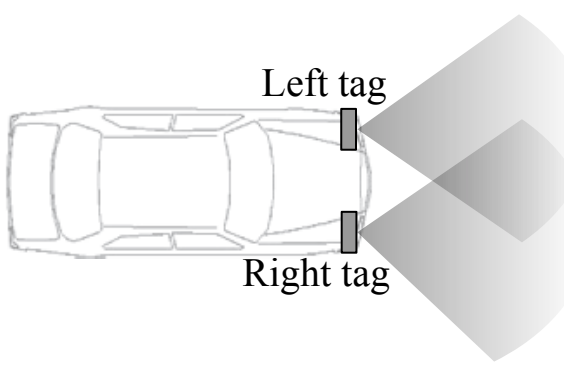


Fig. 7. Two tags are attached at the left and right front of the vehicle respectively to sense the road surface conditions.

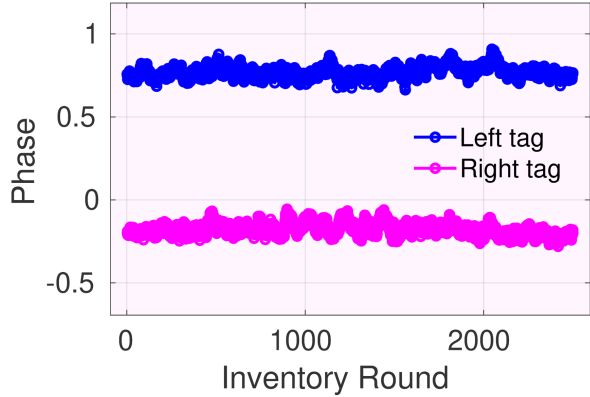


Fig. 8. Left tag and right tag exhibit the different phase readings over time, indicating the different road surface conditions.

line-of-sight propagation channel between the reader and tag can be easily modeled as follows:

$$h_{rt} = h_{tr} = \frac{1}{d_{rt}^2} e^{-j2\pi \frac{d_{rt}}{\lambda} \bmod 2\pi}, \quad (6)$$

where d_{rt} denotes the distance between the reader and tag. We have $h_{rt} = h_{tr}$ due to the geometric symmetry. As we can see, h_{rt} and h_{tr} will be easily calculated with known distance d_{rt} between the reader and tag. Next, we have to compensate the hardware distortion, which can be calibrated once and used for the rest of life [43]. Then, we obtain the expected channel h_{rot} reflected off the road surface.

$$h_{rot} = \frac{h_o}{H' \frac{1}{d_{rt}^2} e^{-j2\pi \frac{d_{rt}}{\lambda} \bmod 2\pi}}, \quad (7)$$

where $H' = h_{Rr} h_{Tr} h_{Rt}$ denotes the calibrated hardware distortion of the reader and tag.

Road surface sensing with signal cancellation algorithm. We present Algorithm 1 to extract the reflection from the road surface. As we can see, we need three steps to extract the reflection from the road surface as follows:

- **Distortion mitigation:** We first need to estimate the impact of hardware distortion and line-of-sight propagation channel between the reader and tag in line-of-sight setting. After pre-calibration, we will obtain H' and equation (6).
- **Backscattered signal extraction:** We deploy our commodity passive RFID system at the front end of the vehicle to sense the road surface conditions. Specifically, we will obtain the received signal at the reader shown in equation (3).
- **Real-time backscattered signal cancellation:** As we drive the vehicle, we collect the received signal at the reader shown in equation (4). We do subtraction in equation (5), which is obtained through subtraction of the consequent and window-sized backscattered signals. Then, we estimate the channel traversing over the road surface from the reader to the tag as shown in equation (7). By doing this, the impact of vehicle's body vibration and the other external reflectors (e.g., curb) could be mitigated, such that we can observe a peak/trough indicating the bump/pothole in the phase profile.



Fig. 9. Experimental setup. The left figure shows RFID reader's two antennas and one tag are attached at the front end of Honda Civic Flutter. The same setup for Honda CR-V Warner can be seen in Fig. 1. The right figure shows RFID reader, PC and smartphone (i.e., used for system performance comparison) are deployed inside of Honda CR-V Warner. Note that RFID reader is connected with two directional antennas (i.e., Tx transmit antenna and Rx receive antenna). We attach RFID tag on the reader's antennas as shown in the zoom-in figure of Fig. 1.

4.4 Enabling Reliable Sensing with Two RFID Tags

Since the commodity passive RFID system is orientation-sensitive and the bumps are randomly distributed on the road surface, it is important to detect these bumps with multiple tags attached to the vehicle for reliable sensing. Considering the beamwidth of the reader's directional antenna (i.e., 105° [4]) and the width of the vehicle and road, we can just attach two tags at the front of the vehicle as shown in Fig. 7. Each tag will be responsible to sense half side of the road surface, which looks like two headlights of the vehicle.

Fig. 8 shows the phase readings over time from two tags. As we can see, two tags present different phase readings, since the road surface conditions are different. We can deploy more tags at the front of the vehicle to achieve reliable and fine-grained road surface sensing. However, we have to consider the low tag reading rate due to the collisions, which will degrade RFID's sensing ability. We will discuss this problem in Sec. 7.

5 IMPLEMENTATION AND EVALUATION

Hardware. We have implemented a prototype of Tago with commodity passive RFID tags and USRP N210 [23] as reader, which is FCC-compliant working at the frequency band of 902-928MHz. We only extract phase and amplitude of the backscattered signal from the reader. Fig. 9 illustrates Tago's hardware components. The circular polarized antennas [4] are connected to the reader, which has antenna gain of 11dBi and beamwidth of 105° . We use different commodity passive RFID tags from atlasRFID store [6] (e.g., ALN-9662, Monza 4D and R6-P [7]) attaching to the front end of the vehicle during the experiments, which are widely used with reading range of 5-15 meters at best [37]. The USRP reader can interrogate the tags and receive the backscattered signals from tags to extract phase and amplitude readings, via the Ethernet cable connecting with a host PC.

Software. The reader's implementation is obtained from the previous work [15], which can enable the RFID communication using USRP N210 as reader. We just use this reader to collect data. Our road surface sensing algorithms are implemented offline with MATLAB for signal processing. The commodity passive RFID system complies with C1G2 standard using slotted ALOHA protocol to interrogate tags. There are two main steps during tag interrogation. At the first step, the activated tags will reply RN16 to the reader for channel access permission (i.e., query step). During query step, the reader will initialize some parameters such as M (i.e., the number of frames/inventory rounds), Q (2^Q indicates the number of time slots in one frame/inventory round), four sessions (i.e., used for multi-reader reading), flags (e.g., SL flag and inventoried flag) and so on. In default, we set $Q=0$, meaning there is one time slot in each frame, since we only have one tag. This can maximize the tag

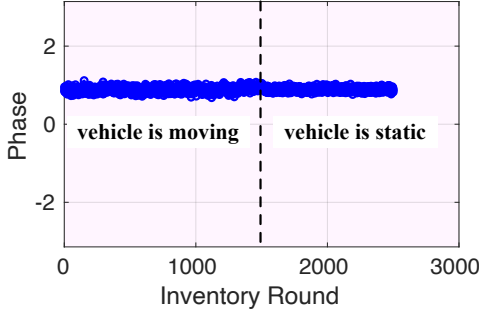


Fig. 10. Phase readings over time, when driving the vehicle on the smooth road with speed of 10mph.

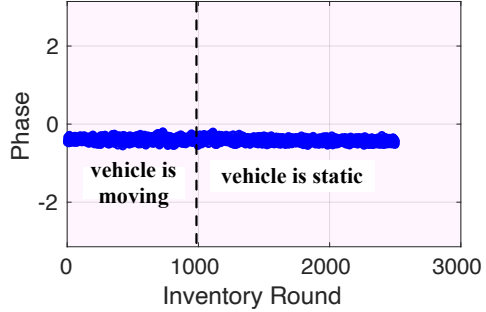


Fig. 11. Phase readings over time, when driving the vehicle on the smooth road with speed of 20mph.

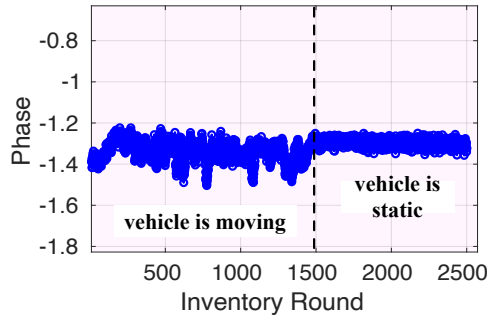


Fig. 12. Phase readings over time, when driving the vehicle on the bumpy road with speed of 10mph.

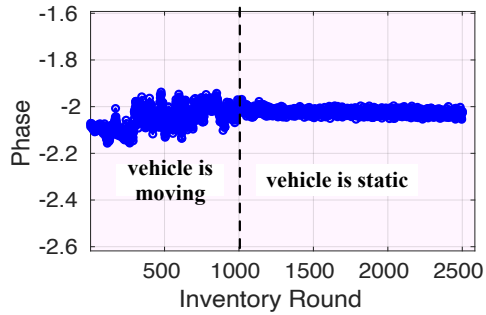


Fig. 13. Phase readings over time, when driving the vehicle on the bumpy road with speed of 20mph.

reading rate (Usually, we use tag reading rate to measure how often we can obtain the channel information in RFID communication). The value of M depends on how long we drive the vehicle (we set it as 5000 by default). The other parameters are set as default value (e.g., zero). At the second step, the reader will chose one tag to communicate and the chosen tag will reply EPC to the reader. The channel information extraction happens in the second step with preamble based channel estimation. The reader will report the phase angle through channel sounding using EPC packets.

Compared approach. We mainly compare the performance of Tago with smartphone-based road surface sensing. We use iphone 7 to measure the data readings from the gyroscope of the smartphone. The smartphone will be deployed and fixed at the different positions inside of the vehicle (e.g., windshield, air-conditioning vents, etc.) as shown in Fig. 9.

Experimental setup. During the experiments, we use different vehicles (e.g., Honda Civic and Honda CRV Warner shown in Fig. 9). We will drive the vehicle on the different road conditions (e.g., bumpy and smooth road) with different speed (e.g. 10mph, 15mph and 20mph). We drive the vehicle in urban (Fig. 26) and residential area (Fig. 28) for road surface sensing.

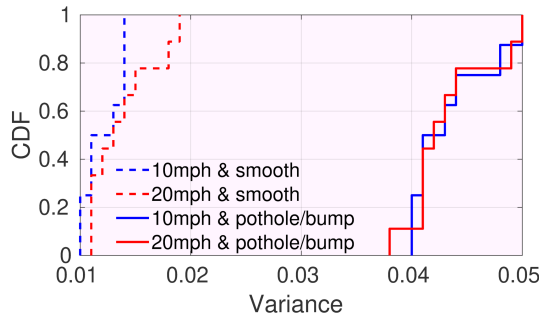


Fig. 14. CDF of phase variance when driving on the smooth and bumpy road with different speed.

6 EXPERIMENTAL RESULTS

6.1 Micro Benchmarks

6.1.1 Effect of Sensing Smooth/Bumpy Road. The different road surface conditions will reflect the backscattered signals differently.

Method. To see the effect of sensing smooth and bumpy road, we drive the vehicle on the smooth and bumpy road respectively with different driving speed. Moreover, we compare the phase readings, when vehicle is moving and static. To do so, we drive the vehicle for a period of time and stop the vehicle to see the variation of phase readings.

Result. Fig. 10 and Fig. 11 show the phase readings over time, when we drive the vehicle on the smooth road with speed of 10mph and 20mph and stop the vehicle during driving. We can see that the phase variation is stable over the time after we stop the vehicle (i.e., the vehicle is static). Fig. 12 and Fig. 13 show the phase readings over time, when we drive the vehicle on bumpy road with speed of 10mph and 20mph and stop the vehicle during driving. As we can see, the phase variation is significant, when we drive the vehicle on the bumpy road. When we stop the vehicle, the phase readings become stable. This is because the road surface conditions will affect the backscattered signals, such that we can use the variation of backscattered signals to sense the bumpy and smooth road surface. Fig. 14 shows the CDF of the phase variance, when we drive the vehicle on smooth and bumpy road with different speed. We can see that the phase variance is consistent, when we drive the vehicle with different speed on the same road surface. When we drive the vehicle on the bumpy road, the phase variance becomes larger in comparison to the phase variance when we drive the vehicle on smooth road. So, Tago can sense the road surface conditions with contact-free commodity passive RFID sensing system.

6.1.2 Impact of Vehicle's Vibration, Passing-by Passengers and Other Vehicles. The backscattered signals are reflected off the different objects around the vehicle such as the vehicle's body, passing-by passengers and vehicles.

Method. To measure the impact of the passing-by passengers and other vehicles, we drive the vehicle on the smooth road at urban area, which can mitigate the impact of road surface condition on the backscattered signals. During the experiments, there are passengers walking on the sidewalk and the other vehicles passing by our vehicle. We will show the phase and amplitude readings over time (i.e., inventory rounds), when we drive the vehicle and the vehicle is static respectively.

Results. Fig. 15 and Fig. 16 show the phase and amplitude readings over inventory rounds, when the vehicle is static and its engine is on. We can see the stable phase and amplitude readings. The vibration of vehicle's engine will not affect backscattered signals. This is because Algorithm 1 has already accounted for the vibration

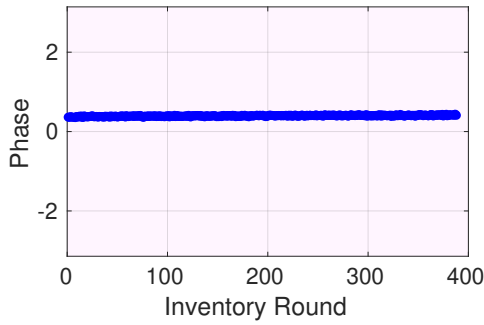


Fig. 15. Phase readings over time, when the vehicle is static and the engine is on.

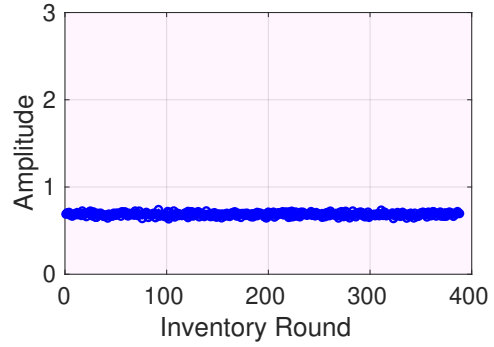


Fig. 16. Amplitude readings over time, when the vehicle is static and the engine is on.

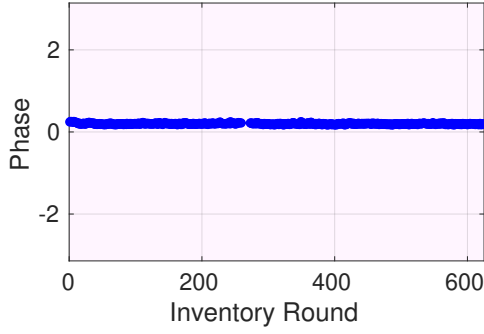


Fig. 17. Phase readings over time, when we drive the vehicle on the smooth road at urban area.

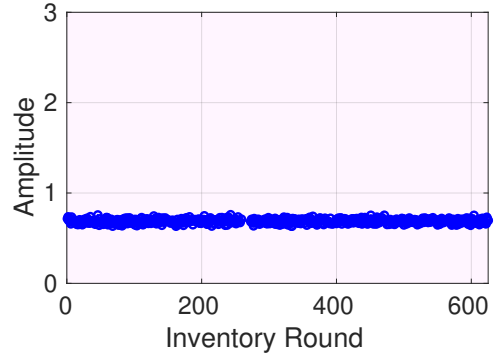


Fig. 18. Amplitude readings over time, when we drive the vehicle on the smooth road at urban area.

of vehicle's body. Then, we drive the vehicle on the smooth road to measure the impact of passing-by passengers and other vehicles. Fig. 17 and Fig. 18 show the phase and amplitude readings over inventory rounds, when we drive the vehicle on the smooth road at urban area. As we can see, the phase and amplitude readings are quite stable, indicating that the passing-by passengers and other vehicles will not affect the backscattered signals. This is because the commodity passive RFID system uses the directional antenna with narrow beamwidth, which will only concentrate the signals in the front of the vehicle. The passing-by passengers and other vehicles will not be in the reader's field-of-view, such that they cannot affect the backscattered signals.

6.1.3 Impact of Pothole Size. The pothole on the road surface may have different size. Intuitively, the bigger pothole is more easier to be detected than the smaller pothole.

Method. To see the impact of pothole size on road surface sensing, we drive the vehicle with speed of 10mph passing by the big pothole (i.e., with size of 85x85x4cm) and small pothole (i.e., with size of 28x28x3.5cm) on the road surface.

Result. Fig. 19 shows the phase readings from the tag, when we drive the vehicle passing the big pothole and small pothole. When we drive the vehicle passing the big pothole, we can see a fat trough in the phase reading profile. But, when we drive the vehicle passing a small pothole, we can see a sharp trough in the phase reading profile. These results indicate that the size of pothole will affect Tag's road surface sensing. Potentially, we can

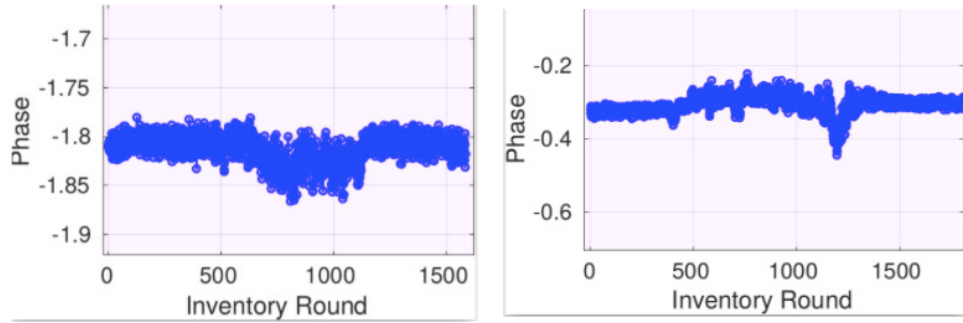


Fig. 19. Left figure shows the phase readings over time, when the vehicle passes the big pothole with size of 85x85x4cm. Right figure shows the phase readings over time, when the vehicle passes the small pothole with size of 28x28x3.5cm.

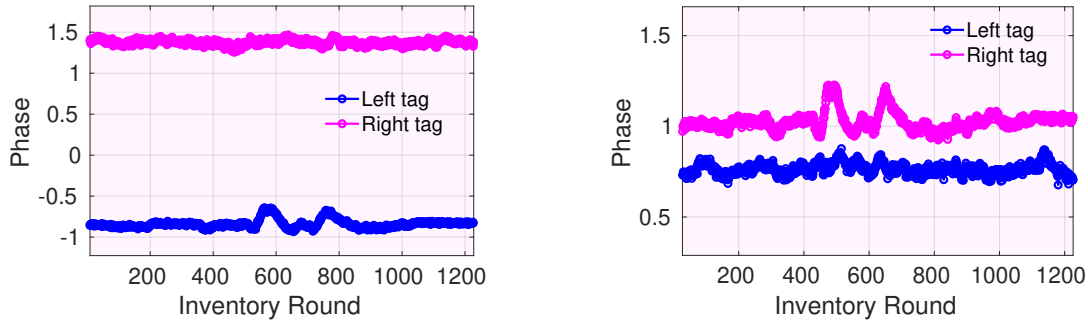


Fig. 20. Pothole located at the left side of the road is detected by the left tag attached on the vehicle.

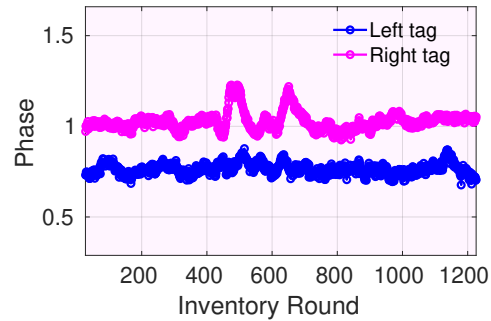


Fig. 21. Pothole located at the right side of the road is detected by the right tag attached on the vehicle.

leverage the phase readings to create the profile of the pothole and bump on the road surface. However, since the tags are just attached at the front end of the vehicle, we can only obtain one dimensional information of the pothole or bump (e.g., width). Profiling the pothole or bump on the road surface (e.g., the length, height and width of the bump or pothole) will be left for our future work.

6.1.4 Effect of Using Two Tags. The commodity passive RFID system employs the directional antenna to concentrate RF signals for long-range RFID communication. And, the potholes or bumps are randomly distributed on the road surface.

Method. To reliably sense the road surface conditions and detect the potholes or bumps on the road surface, we attach two tags at the left and right front end of the vehicle like the vehicle’s headlights. We will first drive the vehicle attached with two tags to pass the pothole on the left side of the road surface. Then, we drive the vehicle attached with two tags to pass the pothole on the right side of the road surface.

Result. Fig. 20 and Fig. 21 show the phase readings of backscattered signals from two tags, when we drive the vehicle passing the pothole located at the left or right side of the road surface. We can see that the phase variation of left tag is significant, when the pothole is located at the left side of the road surface. The phase variation of right tag is significant, when the pothole is located at the right side of the road surface. Since the commodity passive RFID system is orientation-sensitive, only one tag can sense the pothole located at the left or right side of

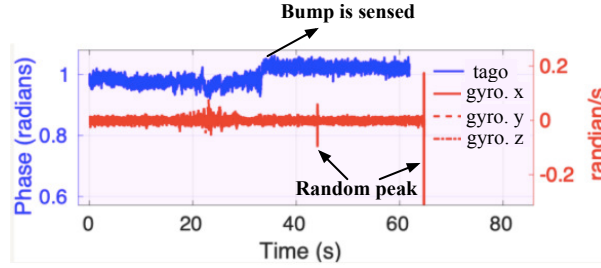


Fig. 22. Phase readings of backscattered signal for the RFID-based contact-free road surface sensing and the rate of rotation measurements from gyroscope for smartphone-based contact road surface sensing.

the road surface. This potentially indicates that the passing-by passengers and other vehicles will not affect the backscattered signals due to the orientation sensitivity of RFID tags. Note, we can deploy more than two tags at the front end of the vehicle to enhance the sensing ability of Tago for road surface sensing. However, we have to consider the low tag reading rate, as we increase the number of tags.

6.2 Contact-Free Road Surface Sensing for Safe Driving

6.2.1 Comparison to the Smartphone-Based Road Surface Sensing. The principle of smartphone-based road surface sensing relies on the MEMS gyroscope or accelerometer to detect the vehicle's body vibration caused by the bump or pothole on the road surface. Therefore, the smartphone-based road surface sensing system requires the vehicle's front tires to hit the bumps or potholes on the road surface to accurately detect them, which is actually violating the goal of safe driving. More details can be found in Sec. 2.

Method. The commodity passive RFID system can provide the contact-free road surface sensing by deploying the reader's antenna and tag at the front end of the vehicle. As shown in Fig. 9, we deploy reader's antenna and RFID tag at the front of the vehicle for contact-free road surface sensing. There is a smartphone fixed at the arbitrary location inside of the vehicle (e.g., windshield). During the experiments, we will drive the vehicle approaching the bump as shown in Fig. 9. But, we will stop the vehicle before the vehicle's front tires touch the bump. By doing this, we can imagine that the sensing data read from the smartphone will not be affected by the bumps, since the vehicle's body does not vibrate. However, the backscattered signals from RFID tags attached at the front end of the vehicle will be affected.

Result. Fig. 22 shows the phase readings from the RFID tag and the rate of rotation measurements from gyroscope embedded in the smartphone. We can see that the phase readings are abruptly changed at 35 seconds. However, the rate of rotation measurements from the gyroscope keeps stable over time during the experiments. Therefore, we can claim that the smartphone-based road surface sensing indeed requires vehicle's body vibration caused by the bumps or potholes on the road surface, which cannot achieve safe driving. However, the commodity passive RFID system can achieve contact-free sensing, which does not require the vehicle's tires to touch the bumps or potholes due to the fact of RF signals propagation. In comparison to the smartphone-based road surface sensing, Tago indeed achieves safe driving. Therefore, we believe commodity passive RFID system is a good choice to achieve road surface sensing for safe and economic driving due to its low-cost (considering the smartphone can be the reader [5, 8]), small form-factor and contact-free sensing.

6.2.2 Effect of Contact-Free Road Surface Sensing with Tago. We have shown the contact-free sensing using Tago in comparison to the smartphone-based road surface sensing, which will enable the safe driving. Then, the problem becomes how far Tago can detect the pothole/bump on the road surface.

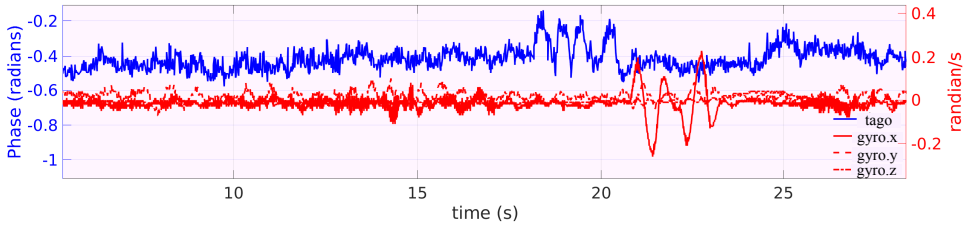


Fig. 23. Phase readings from the tag and gyroscope data from the smartphone, when we drive the vehicle in the speed of 10mph passing the bump on the road surface.

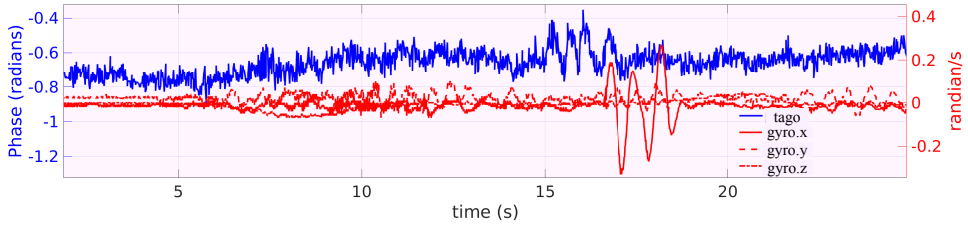


Fig. 24. Phase readings from the tag and gyroscope data from the smartphone, when we drive the vehicle in the speed of 15mph passing the bump on the road surface.

Method. Here, we measure the phase readings from the tag and the data from the gyroscope of the smartphone, when we drive the vehicle in different speed. We will see how far away our Tago can sense the bump on the road surface in comparison to using the smartphone.

Result. Fig. 23 shows the phase readings from tag and gyroscope data from smartphone, when we drive the vehicle in the speed of 10mph passing the bump on the road surface. As we can see, Tago can sense the bump on the road surface about 2.2 seconds earlier than using the smartphone to sense the bump. Therefore, Tago can sense the bump on the road surface in contact-free way, which can allow about 2.2 seconds for the vehicular system to react to the hazardous road conditions. Fig. 24 shows the phase readings from tag and gyroscope data from smartphone, when we drive the vehicle in the speed of 15mph passing the bump on the road surface. We can see that Tago can sense the road surface about 1.6 seconds earlier than using the smartphone to sense the bump. So, the vehicular system has about 1.6 seconds to react to the hazardous road conditions. Fig. 25 shows the phase readings from tag and gyroscope data from smartphone, when we drive the vehicle in the speed of 20mph passing the bump on the road surface. As we can see, Tago can sense the road surface about 1.0 seconds earlier than using the smartphone to sense the bump. So, the vehicular system has about 1.0 seconds to react to the hazardous road conditions. The above results indicate that Tago can achieve the goal of safe driving due to its contact-free sensing.

6.3 Case Study

In this subsection, we measure the accuracy of sensing the bumps on the road surface using Tago, when we drive the vehicle on the roadways at the urban and residential area respectively.

Method. To see the performance of Tago on roadways, we drive the vehicle at residential community and urban area. There are several bumps on the road surface. Our Tago is responsible to detect these bumps on the road surface.

Result. Fig. 26 shows the detected bumps along the driving path at the urban area. Fig. 28 shows the detected bumps along the driving path at residential community. We also indicate the ground-truth location of the bumps

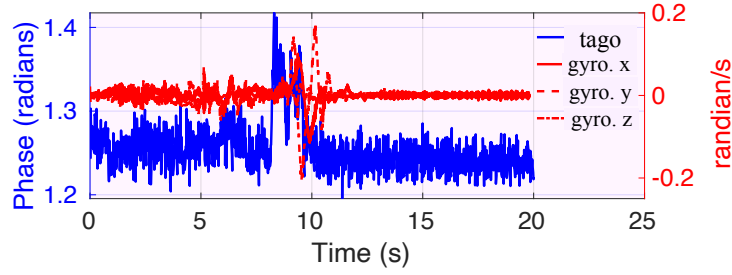


Fig. 25. Phase readings from the tag and gyroscope data from the smartphone, when we drive the vehicle in the speed of 20mph passing the bump on the road surface.

(i.e., blue dots) along the driving path. The detected bumps are indicated in the figures with the red stars. As we can see, Tago can accurately detect the bumps on the road surface. Fig. 27 and Fig. 29 show the phase readings from the tag and gyroscope data from the smartphone, when we drive the vehicle at urban area shown in Fig. 26 and residential area shown in Fig. 28 respectively. We drive the vehicle in the speed of around 15mph. The road surface between two bumps is quite smooth in these two areas. So, we can see that both of the phase readings and gyroscope data are quite stable, when we drive on the smooth road. Furthermore, we have two observations as follows. First, Tago can accurately detect the bumps on the road surface. Second, Tago can sense the bumps on the road surface earlier than using the smartphone to sense the bumps, thereby the contact-free road surface sensing is achieved.

7 DISCUSSION

7.1 Fine-Grained Road Surface Sensing

Our paper aims to detect the road surface conditions. Specifically, the bumps or potholes on the road surface can be detected based on the backscattered signals reflected off the road surface. For fine-grained road surface sensing, we expect to differentiate the bumps and potholes on the road surface and sense the geometry of these bumps/potholes. These fine-grained road surface information can be used for road maintenance analysis. To do so, the straightforward idea is using some advanced sensors (e.g., camera, Lidar and radar sensors). We need deploy multiple sensors on the vehicle to obtain the 3D geometry of bump/pothole. Can we use RFID tags to sense the fine-grained road surface information? To differentiate the pothole and bump on the road surface, we can use one RFID tag deployed in the front of the vehicle and leverage the machine learning algorithm to do classification based on the backscattered signals reflected off the road surface. To characterize 3D geometry of bump or pothole on the road surface, we probably need to deploy multiple tags at the front end of vehicle. But, we cannot make sure that the backscattered signals from the tag array can capture the different parts of the bump or pothole for 3D geometry sensing. Furthermore, using tag array will introduce extra processing latency, since commodity passive RFID system interrogates tag with slotted ALOHA protocol. The collision-free tag interrogation protocols (e.g., parallel decoding) can be used. But, these protocols have downsides (e.g., they can only work with tens of tags and require the hardware modification of tag or reader), which constrain them to be widely deployed.

7.2 Long Range Sensing with Active Tags and Distributed Beamforming

The passive RFID tag is limited by its communication range. To increase the communication range, we can use the active tags. But, these active tags require the battery replacement regularly. Recently, we notice that the tunnelling RFID tag can achieve long range sensing, which is not commercialized. In comparison to these active tags and customized tags, passive RFID tags are ubiquitous. We can enhance communication range of passive

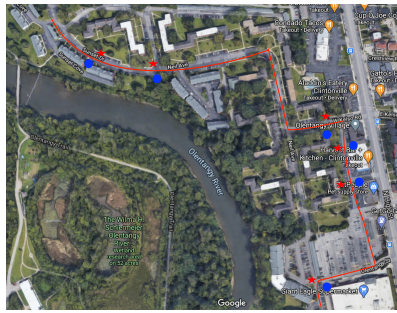


Fig. 26. Driving vehicle at the urban area. The red line shows the driving path. The red star indicates the detected bumps using Tago. The blue dot indicates the ground-truth bumps along the driving path.

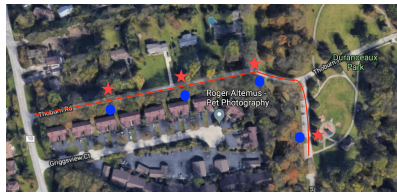


Fig. 28. Driving vehicle at the residential area. The red line shows the driving path. The red star indicates the detected bumps using Tago. The blue dot indicates the ground-truth bumps along the driving path.

RFID tags with distributed beamforming using multiple readers like PushID [37]. To see how PushID can work for Tago, we believe that there are two design spaces. The straightforward idea of applying PushID to Tago is deploying multiple readers on the vehicle, and these readers can collaborate with each other to do beamforming to activate the tag. However, this approach seems bulky due to the size of reader's directional antenna and the vehicle. The another way is to deploy one reader and one tag for each vehicle. Then, the tag is activated by the readers deployed on the adjacent vehicles through opportunistic beamforming. As the proliferation of connected and automated vehicle (CAV) and edge computing, the readers at the different vehicles can collaborate with each other through Internet backbone. However, this deployment has one downside. It will introduce collisions across the readers, which requires the readers deployed at different vehicles to collaborate with each other for collision resolving. Note that the limited communication range is not inherited from Tago's design. Our algorithm and design can be extended to the general low-power backscatter tag.

7.3 Crowdsourcing-Based Road Surface Information Sharing

Due to the proliferation of connected and automated vehicle (CAV), the vehicles collaborate with each other and connect with the remote cloud. This CAV architecture can further enhance Tago's design and deployment. Imagine the road surface information collected by one vehicle using Tago can be shared with other vehicles through Internet backbone. The other vehicles will obtain the road surface information directly from google map. Note the current satellite-based navigation system cannot show the road surface information to the drivers. The

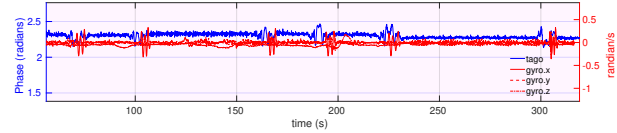


Fig. 27. Phase readings from the tag and gyroscope data from the smartphone, when we drive the vehicle in the urban area shown in Fig. 26.

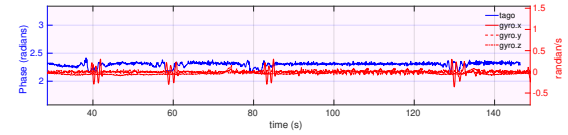


Fig. 29. Phase readings from the tag and gyroscope data from the smartphone, when we drive the vehicle in the residential area shown in Fig. 28.

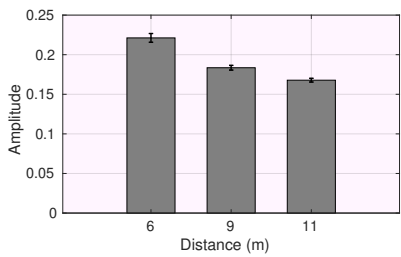


Fig. 30. Amplitude of backscattered signals over different tag-reader distance.

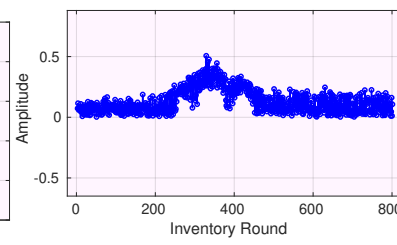


Fig. 31. Amplitude readings of backscattered signals, when people perform the gesture 10 meters away from Tago's setup.

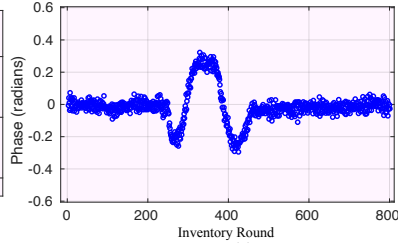


Fig. 32. Phase readings of backscattered signals, when people perform the gesture 10 meters away from Tago's setup.

data processing and analysis can be moved to the cloud to relieve the computation at the vehicle. One downside of this scheme is the communication latency at the Internet backbone, especially for highly mobile vehicles. We hope this barrier can be tackled, as 5G becomes ubiquitous. Note that as more vehicles employ Tago for road surface sensing and the traffic becomes crowded on the road, the collisions across the reader from different vehicles may degrade the performance of road surface sensing. We hope the collision-free schemes for RFID communication could solve this problem. Moreover, the directivity of Tago will mitigate the inter-reader interference.

7.4 Communication Range and Sensing Range of Passive RFIDs

In commodity passive RFID system, the tag is battery-free, which can be activated by the external reader. So, the communication range is highly depending on the reader's capability to illuminate the tag. So, the reader is usually instrumented with the directional antenna to concentrate the signals for powering up the tag. To fully power up the tag, the reader transmits the constant continuous wave. In our case, since we attach the tag on the reader's antenna, the tag will always be activated. This means that the tag can always communicate with the reader. Tago relies on the backscattered signals reflected off the road surface to sense the bumps. The sensing range is highly depending on how far the transmitted RF signals from the reader can arrive and be received at the reader after being reflected off the road surface and modulated by the tag. Intuitively, the sensing range will be larger than the communication range, since the tag needs to be activated when the power of impinged RF signals is larger than a threshold consistently. However, in RFID-based sensing, the channel state information of backscattered signals are extracted from the EPC packets. In another words, the RF signals reflected off the road surface need to be modulated by the tag for preamble-based channel estimation to extract the desired channel for road surface sensing. Therefore, the tag needs to be activated and communicate with the reader, such that we can extract the phase or amplitude information to do sensing. In this regard, the sensing range is same as the communication range in RFID-based sensing. We also do the following micro-benchmark experiments to show the communication and sensing range of Tago.

First, we attach reader's antennas at the front end of the vehicle. We do not attach the tag to the reader's antenna like Tago's setup. We measure the amplitude of the backscattered signals, when we put tag 6, 9 and 11 meters away from the reader's antennas in front of the vehicle. Fig. 30 shows the amplitude of backscattered signals, when the tag is deployed 6, 9 and 11 meters away from the reader's antennas. We can see that the amplitude decreases as the tag-antenna distance increases. The reader can still read the tag, even though the tag is 11 meters away from the reader. This experiment indicates that the RFID system's communication range can be more than 10 meters. This indicates that the sensing range of Tago could be larger than 10 meters. Next, we will showcase the reader can indeed capture the variation 10 meters far away from the Tago's setup.

We directly show 10m sensing range of Tago through a case study. We evaluate the sensing range in Tago's setup. We attach reader's antennas at the front end of the vehicle, and the tag is attached on the reader's antenna. Then, we ask one person who is 10 meters away from Tago's setup to perform the gesture in front of the vehicle. Tago will process the backscattered signals. Fig. 31 and Fig. 32 show the amplitude and phase readings over time, when people perform the gesture 10 meters away from Tago. As we can see, Tago has the sensing range of 10 meters.

8 CONCLUSION

In this paper, we propose a system, Tago that can sense the road surface conditions with commodity passive RFID system. Instead of deploying the reader or tags on the existing infrastructure (e.g., lamp post and roadways), we deploy the reader inside of the vehicle and the tag will be attached at the front end of the vehicle to achieve contact-free sensing. We comprehensively analyse Tago's settings. Then, we propose the road surface sensing with the signal cancellation algorithm to achieve the contact-free road surface sensing. The extensive experiments show the efficiency of Tago on road surface sensing in comparison to the state-of-the-art smartphone-based road surface sensing.

ACKNOWLEDGMENTS

We are grateful to the anonymous reviewers for their insightful feedback. This work was supported by the National Science Foundation under Grant 1618520.

REFERENCES

- [1] Automatic road analyzer. <https://www.wtae.com/article/aran-on-the-prowl-automatic-road-analyzer-gathers-information-to-map-future-state-road-repairs-1/7462861>.
- [2] Understanding the Link Between Unsafe Road Conditions and Car Accidents. <https://www.makeroadssafe.org/understanding-the-link-between-unsafe-road-conditions-and-car-accidents/>.
- [3] Omid Abari, Deepak Vasisht, Dina Katabi, and Anantha Chandrakasan. 2015. Caraoke: An e-toll transponder network for smart cities. In *Proceedings of the 2015 ACM Conference on Special Interest Group on Data Communication*. 297–310.
- [4] Alien. 2020. ALR-8697-8. <https://www.alientechnology.com/products/antennas/alr-8697-8/>.
- [5] Zhenlin An, Qiongzheng Lin, and Lei Yang. 2018. Cross-frequency communication: Near-field identification of uhf rfids with wifi!. In *Proceedings of the 24th Annual International Conference on Mobile Computing and Networking*. 623–638.
- [6] atlasRFIDstore. 2020. Commodity passive RFID tags. <https://www.atlasrfidstore.com/rfid-tag-sample-pack-uhf-passive/>.
- [7] atlasRFIDstore. 2020. Commodity Passive RFID tags. <https://www.atlasrfidstore.com/rfid-tags/>.
- [8] Joshua F Ensworth and Matthew S Reynolds. 2015. Every smart phone is a backscatter reader: Modulated backscatter compatibility with bluetooth 4.0 low energy (ble) devices. In *2015 IEEE international conference on RFID (RFID)*. IEEE, 78–85.
- [9] Jakob Eriksson, Lewis Girod, Bret Hull, Ryan Newton, Samuel Madden, and Hari Balakrishnan. 2008. The pothole patrol: using a mobile sensor network for road surface monitoring. In *Proceedings of the 6th international conference on Mobile systems, applications, and services*. 29–39.
- [10] Junfeng Guan, Sohrab Madani, Suraj Jog, Saurabh Gupta, and Haitham Hassanieh. 2020. Through Fog High-Resolution Imaging Using Millimeter Wave Radar. In *Proceedings of the IEEE/CVF Conference on Computer Vision and Pattern Recognition*. 11464–11473.
- [11] Abhishek Gupta, Shaohan Hu, Weida Zhong, Adel Sadek, Lu Su, and Chunming Qiao. 2020. Road Grade Estimation Using Crowd-Sourced Smartphone Data. In *2020 19th ACM/IEEE International Conference on Information Processing in Sensor Networks (IPSN)*. IEEE, 313–324.
- [12] Unsoo Ha, Junshan Leng, Alaa Khaddaj, and Fadel Adib. 2020. Food and Liquid Sensing in Practical Environments using RFIDs. In *17th {USENIX} Symposium on Networked Systems Design and Implementation ({NSDI} 20)*. 1083–1100.
- [13] Jens Jauch, Johannes Masino, Tim Staiger, and Frank Gauterin. 2017. Road grade estimation with vehicle-based inertial measurement unit and orientation filter. *IEEE Sensors Journal* 18, 2 (2017), 781–789.
- [14] Haojian Jin, Zhijian Yang, Swarun Kumar, and Jason I Hong. 2018. Towards wearable everyday body-frame tracking using passive rfids. *Proceedings of the ACM on Interactive, Mobile, Wearable and Ubiquitous Technologies* 1, 4 (2018), 1–23.
- [15] Nikos Kargas, Fanis Mavromatis, and Aggelos Bletsas. 2015. Fully-coherent reader with commodity SDR for Gen2 FM0 and computational RFID. *IEEE Wireless Communications Letters* 4, 6 (2015), 617–620.

- [16] Keiko Katsuragawa, Ju Wang, Ziyang Shan, Ningshan Ouyang, Omid Abari, and Daniel Vogel. 2019. Tip-Tap: Battery-free Discrete 2D Fingertip Input. In *Proceedings of the 32nd Annual ACM Symposium on User Interface Software and Technology*. 1045–1057.
- [17] Rushil Khurana and Mayank Goel. 2020. Eyes on the Road: Detecting Phone Usage by Drivers Using On-Device Cameras. In *Proceedings of the 2020 CHI Conference on Human Factors in Computing Systems*. 1–11.
- [18] Martin Laurenzis, Frank Christnacher, Emmanuel Bacher, Nicolas Metzger, Stéphane Schertzer, and Thomas Scholz. 2011. New approaches of three-dimensional range-gated imaging in scattering environments. In *Electro-Optical Remote Sensing, Photonic Technologies, and Applications V*, Vol. 8186. International Society for Optics and Photonics, 818603.
- [19] Jaeyoung Lee, BooHyun Nam, and Mohamed Abdel-Aty. 2015. Effects of pavement surface conditions on traffic crash severity. *Journal of Transportation Engineering* 141, 10 (2015), 04015020.
- [20] Yunfei Ma, Nicholas Selby, and Fadel Adib. 2017. Minding the billions: Ultra-wideband localization for deployed rfid tags. In *Proceedings of the 23rd Annual International Conference on Mobile Computing and Networking*. 248–260.
- [21] Prashanth Mohan, Venkata N Padmanabhan, and Ramachandran Ramjee. 2008. Nericell: rich monitoring of road and traffic conditions using mobile smartphones. In *Proceedings of the 6th ACM conference on Embedded network sensor systems*. 323–336.
- [22] Kun Qian, Shilin Zhu, Xinyu Zhang, and Li Erran Li. 2021. Robust Multimodal Vehicle Detection in Foggy Weather Using Complementary Lidar and Radar Signals. In *Proceedings of the IEEE/CVF Conference on Computer Vision and Pattern Recognition*. 444–453.
- [23] Ettus Research. 2020. USRP N210. <https://www.ettus.com/product/details/UN210-KIT/>.
- [24] Guy Satat, Matthew Tancik, and Ramesh Raskar. 2018. Towards photography through realistic fog. In *2018 IEEE International Conference on Computational Photography (ICCP)*. IEEE, 1–10.
- [25] Fatjon Seraj, Berend Jan van der Zwaag, Arta Dilo, Tamara Luarasi, and Paul Havinga. 2015. RoADS: A road pavement monitoring system for anomaly detection using smart phones. In *Big data analytics in the social and ubiquitous context*. Springer, 128–146.
- [26] Henry M Stommel, Dennis W Moore, and Dennis W Moore. 1989. *An introduction to the Coriolis force*. Columbia University Press.
- [27] Jsun2020allergie Wei Sun and Kannan Srinivasan. [n. d.]. Allergie: Relative Vehicular Localization with Commodity RFID System. In *2020 IEEE International Conference on RFID (RFID)*. IEEE, 1–8.
- [28] Tesla. 2020. Autonomous vehicle. <https://www.tesla.com/>.
- [29] Saurabh Tiwari, Ravi Bhandari, and Bhaskaran Raman. 2020. Roadcare: a deep-learning based approach to quantifying road surface quality. In *Proceedings of the 3rd ACM SIGCAS Conference on Computing and Sustainable Societies*. 231–242.
- [30] Jue Wang, Fadel Adib, Ross Knepper, Dina Katabi, and Daniela Rus. 2013. RF-compass: Robot object manipulation using RFIDs. In *Proceedings of the 19th annual international conference on Mobile computing & networking*. 3–14.
- [31] Ju Wang, Liqiong Chang, Shourya Aggarwal, Omid Abari, and Srinivasan Keshav. 2020. Soil moisture sensing with commodity RFID systems. In *Proceedings of the 18th International Conference on Mobile Systems, Applications, and Services*. 273–285.
- [32] Jue Wang and Dina Katabi. 2013. Dude, where's my card? RFID positioning that works with multipath and non-line of sight. In *Proceedings of the ACM SIGCOMM 2013 conference on SIGCOMM*. 51–62.
- [33] Ju Wang, Jianyan Li, Mohammad Hosseini Mazaheri, Keiko Katsuragawa, Daniel Vogel, and Omid Abari. 2020. Sensing finger input using an RFID transmission line. In *Proceedings of the 18th Conference on Embedded Networked Sensor Systems*. 531–543.
- [34] Jingxian Wang, Chengfeng Pan, Haojian Jin, Vaibhav Singh, Yash Jain, Jason I Hong, Carmel Majidi, and Swarun Kumar. 2019. RFID Tattoo: A Wireless Platform for Speech Recognition. *Proceedings of the ACM on Interactive, Mobile, Wearable and Ubiquitous Technologies* 3, 4 (2019), 1–24.
- [35] Jue Wang, Deepak Vasishth, and Dina Katabi. 2014. RF-IDraw: virtual touch screen in the air using RF signals. *ACM SIGCOMM Computer Communication Review* 44, 4 (2014), 235–246.
- [36] Ju Wang, Jie Xiong, Xiaojiang Chen, Hongbo Jiang, Rajesh Krishna Balan, and Dingyi Fang. 2017. TagScan: Simultaneous target imaging and material identification with commodity RFID devices. In *Proceedings of the 23rd Annual International Conference on Mobile Computing and Networking*. 288–300.
- [37] Jingxian Wang, Junbo Zhang, Rajarshi Saha, Haojian Jin, and Swarun Kumar. 2019. Pushing the range limits of commercial passive RFIDs. In *16th {USENIX} Symposium on Networked Systems Design and Implementation ({NSDI} 19)*. 301–316.
- [38] Yinsong Wang, Yajie Zou, Kristian Henrickson, Yinhai Wang, Jinjun Tang, and Byung-Jung Park. 2017. Google Earth elevation data extraction and accuracy assessment for transportation applications. *PloS one* 12, 4 (2017), e0175756.
- [39] waymo. 2020. Autonomous vehicle. <https://waymo.com/>.
- [40] Teng Wei and Xinyu Zhang. 2016. Gyro in the air: tracking 3D orientation of batteryless internet-of-things. In *Proceedings of the 22nd Annual International Conference on Mobile Computing and Networking*. 55–68.
- [41] Binbin Xie, Jie Xiong, Xiaojiang Chen, and Dingyi Fang. 2020. Exploring commodity RFID for contactless sub-millimeter vibration sensing. In *Proceedings of the 18th Conference on Embedded Networked Sensor Systems*. 15–27.
- [42] Lei Yang, Yekui Chen, Xiang-Yang Li, Chaowei Xiao, Mo Li, and Yunhao Liu. 2014. Tagoram: Real-time tracking of mobile RFID tags to high precision using COTS devices. In *Proceedings of the 20th annual international conference on Mobile computing and networking*. 237–248.

- [43] Lei Yang, Qiongzheng Lin, Xiangyang Li, Tianci Liu, and Yunhao Liu. 2015. See through walls with COTS RFID system!. In *Proceedings of the 21st Annual International Conference on Mobile Computing and Networking*. 487–499.
- [44] Panlong Yang, Yuanhao Feng, Jie Xiong, Ziyang Chen, and Xiang-Yang Li. 2020. RF-Ear: Contactless Multi-device Vibration Sensing and Identification Using COTS RFID. In *IEEE INFOCOM 2020-IEEE Conference on Computer Communications*. IEEE, 297–306.
- [45] Xiaobin Zhang, Liangfei Xu, Jianqiu Li, and Minggao Ouyang. 2013. Real-time estimation of vehicle mass and road grade based on multi-sensor data fusion. In *2013 IEEE Vehicle Power and Propulsion Conference (VPPC)*. IEEE, 1–7.
- [46] Weida Zhong, Qiuling Suo, Fenglong Ma, Yunfei Hou, Abhishek Gupta, Chunming Qiao, and Lu Su. 2019. A Reliability-Aware Vehicular Crowdsensing System for Pothole Profiling. *Proceedings of the ACM on Interactive, Mobile, Wearable and Ubiquitous Technologies* 3, 4 (2019), 1–26.